

European temperature responses to blocking and ridge regional patterns

Pedro M. Sousa¹  · Ricardo M. Trigo¹ · David Barriopedro^{2,3} · Pedro M. M. Soares¹ · João A. Santos⁴

Received: 9 August 2016 / Accepted: 3 March 2017 / Published online: 24 March 2017
© Springer-Verlag Berlin Heidelberg 2017

Abstract Blocking occurrence and its impacts on European temperature have been studied in the last decade. However, most previous studies on blocking impacts have focused on winter only, disregarding its fingerprint in summer and differences with other synoptic patterns that also trigger temperature extremes. In this work, we provide a clear distinction between high-latitude blocking and subtropical ridges occurring in three sectors of the Euro-Atlantic region, describing their climatology and consequent impacts on European temperature during both winter and summer. Winter blocks (ridges) are generally associated to colder (warmer) than average conditions over large regions of Europe, in some areas with anomalies larger than 5 °C, particularly for the patterns occurring in the Atlantic and Central European sectors. During summer, there is a more regional response characterized by above average temperature for both blocking and ridge patterns, especially those occurring in continental areas, although negative temperature anomalies persist in southernmost areas during

blocking. An objective analysis of the different forcing mechanisms associated to each considered weather regime has been performed, quantifying the importance of the following processes in causing the temperature anomalies: horizontal advection, vertical advection and diabatic heating. While during winter advection processes tend to be more relevant to explain temperature responses, in summer radiative heating under enhanced insolation plays a crucial role for both blocking and ridges. Finally, the changes in the distributions of seasonal temperature and in the frequencies of extreme temperature indices were also examined for specific areas of Europe. Winter blocking and ridge patterns are key drivers in the occurrence of regional cold and warm extreme temperatures, respectively. In summer, they are associated with substantial changes in the frequency of extremely warm days, but with different signatures in southern Europe. We conclude that there has been some misuse of the traditional blocking definition in the attribution of extreme events.

Electronic supplementary material The online version of this article (doi:[10.1007/s00382-017-3620-2](https://doi.org/10.1007/s00382-017-3620-2)) contains supplementary material, which is available to authorized users.

✉ Pedro M. Sousa
ppsousa@fc.ul.pt

¹ Instituto Dom Luiz (IDL), Faculdade de Ciências, Universidade de Lisboa, 1749-016 Lisboa, Portugal

² Departamento de Física de la Tierra II, Facultad de Ciencias Físicas, Universidad Complutense de Madrid, Madrid, Spain

³ Instituto de Geociencias (IGEO), CSIC-UCM, Madrid, Spain

⁴ Centre for the Research and Technology of Agro-Environmental and Biological Sciences, CITAB, Universidade de Trás-os-Montes e Alto Douro, UTAD, Vila Real, Portugal

Keywords Blocking · Ridges · Temperature · Europe · Extremes · Synoptic meteorology

1 Introduction

Anomalous temperature episodes are one of the most widely addressed topics in climatological studies, and numerous works have been published in the last decades concerning this subject in Europe, at both continental and regional scales. They cover a wide range of sub-topics, ranging from winter cold spells to summer heatwaves (e.g. Santos et al. 2006; Cattiaux et al. 2010; Andrade et al. 2012; Simolo et al. 2012; Monteiro et al. 2013; Lowe et al. 2015), heatwave-related mortality (García-Herrera

et al. 2005; Trigo et al. 2009; Muthers et al. 2010; Green et al. 2016), forest fires (Pereira et al. 2005; Marcos et al. 2014; Sousa et al. 2015), drought occurrence and agricultural management (Bastos et al. 2014; Gouveia et al. 2016), amongst other topics. The physical and dynamical mechanisms that trigger such extreme episodes are interpreted with very distinct methodologies. In this sense, an increasing number of studies are focusing on the contribution from large-scale dynamics and mid-latitude synoptic circulation patterns to the occurrence of these anomalously cold/warm temperature episodes (e.g. Andrade et al. 2012; Cattiaux et al. 2012; Li et al. 2013; Pfahl 2014).

In the context of climatic change, trends in global mean temperature have been accompanied by an increase of warm extreme temperature events (Fischer and Knutti 2015), which has not been offset by the hiatus or slowdown in global mean temperature rise of the last 15 years (Seneviratne et al. 2014). These recent trends do not only indicate a thermodynamic forcing, but also changes in the frequency of occurrence of mid-latitude circulation patterns (Horton et al. 2015), thus stressing the need of characterizing their associated impacts.

Regarding European winter cold spells, there is a wide consensus on the critical role played by atmospheric blocking episodes over large sectors of the European continent. In works such as Trigo et al. (2004), Cattiaux et al. (2010), Sillmann et al. (2011), de Vries et al. (2012) or Pfahl (2014), the role of blocking structures in transporting cold air from higher latitudes or from cold landmasses becomes quite clear. Other studies have undertaken a deeper analysis of some specific European winter cold spells, as well as of their associated synoptic context, and have also addressed feedback processes that may amplify the resulting anomalies, such as Eurasian autumn snow-cover anomalies (García-Herrera and Barriopedro 2006; Cohen 2011). The interplay between Rossby wave-breaking and jet stream regimes (Woollings et al. 2011), or the occurrence of Sudden Stratospheric Warmings (Barriopedro and Calvo 2014; Liu et al. 2014), are potential mediators of blocking activity, and hence, important precursors of cold events. Episodes like the extensive cold spell which occurred on the later stages of the previously mild winter of 2012 (WMO 2012) are pertinent examples of the relevance of complex feedback processes in triggering significant European cold blasts.

Blocking has also been associated with extremely warm episodes in summer (Buehler et al. 2011; Andrade et al. 2012; Pfahl 2014). However, using the well-known 2003 heatwave in Europe as an example, García-Herrera et al. (2010) stressed that there is some overstatement when attributing these episodes to standard definitions of atmospheric blocking—high-latitude quasi-stationary anticyclones associated with a reversal of the prevailing westerly

flow (e.g., Rex 1950a, b; Treidl et al. 1981; Barriopedro et al. 2006, 2010a). These weather systems are indeed in clear association with summer heat episodes over European mid/high-latitudes (e.g. Barriopedro et al. 2011; Pfahl 2014). However, this is not the case for southern European sectors, where high-latitude blocks are frequently associated with colder than average temperatures throughout the year. Therefore, there is a clear need to distinguish high-latitude blocking structures from low-latitude systems, including the extensions of sub-tropical high pressure systems, commonly denominated as sub-tropical ridges. Unlike canonical blocking systems, sub-tropical ridges do not have the necessary condition of a wave-breaking occurrence (Woollings et al. 2011; Masato et al. 2011; Santos et al. 2013). They manifest as relatively narrow bands of positive anomalies of geopotential height extending from sub-tropical latitudes towards southern Europe and often reaching higher latitudes. Although sub-tropical ridges can be precursors of wave-breaking and subsequent blocking (Altenhoff et al. 2008; Masato et al. 2011; Davini et al. 2012), their impacts on European surface temperatures are rather different from those of high-latitude blocks.

García-Herrera et al. (2005) briefly introduced the importance of sub-tropical ridging patterns on extreme summer temperatures over Iberia. Other studies have analyzed ridge patterns over Europe and their influence on rainfall regimes and droughts in southwestern Europe (Santos et al. 2009, 2013). However, there are no systematic studies aiming to characterize and distinguish the impacts on European temperature due to blocking and ridge patterns, at both regional and seasonal scales. In this paper, we characterize the local and regional European temperature responses associated with blocking and ridging patterns occurring over different locations of the Euro-Atlantic sector and on different seasons. We also clarify some of the referred ambiguity on the impacts' attribution to these weather systems. More specifically, the main objectives are to: (1) distinguish blocking and ridge structures with objective detection schemes; (2) characterize the seasonal impacts of these patterns, considering their specific location, on European surface temperature (including extremes); (3) objectively quantify the contribution and seasonality of the main physical mechanisms involved in the regional temperature anomalies associated to blocking and ridging regimes.

2 Data and methods

2.1 Meteorological data

Maximum and minimum near-surface temperatures (at 2 m above the ground, T2m hereafter) are considered for the

period spanning between 1950 and 2012 from the E-OBS dataset (Haylock et al. 2008). This high-resolution gridded dataset is provided by the European Climate Assessment and Dataset (ECA&D) project, and is available on a daily basis and on a horizontal resolution of 0.25° latitude \times 0.25° longitude. This regular grid is obtained by interpolating observations from local meteorological stations. Despite the overall good quality of this dataset, it must be acknowledged that it has some caveats in areas where the spatial distribution of stations is sparser (e.g., Kyselý and Plavcová 2010). Moreover, the E-OBS temperature dataset suffers from other limitations such as inhomogeneities in input records, statistical interpolation errors and “heat island” effects (Hofstra et al. 2009; van der Schrier et al. 2013).

The NCEP/NCAR reanalysis daily dataset is also used (Kalnay et al. 1996), at a 2.5° latitude \times 2.5° longitude horizontal resolution for the same period. The following mean daily fields are selected: 500 hPa geopotential height (Z500); 850 hPa temperature, omega-vertical velocity and horizontal wind components; upward, downward and net long-wave and short-wave surface fluxes; and total cloud cover. The Z500 field was used to compute the blocking (Barriopedro et al. 2006) and ridge days catalogues separately, as described below. These two different dynamical indicators will be used to distinguish the impacts of anomalous geopotential fields at different European sectors (see next section).

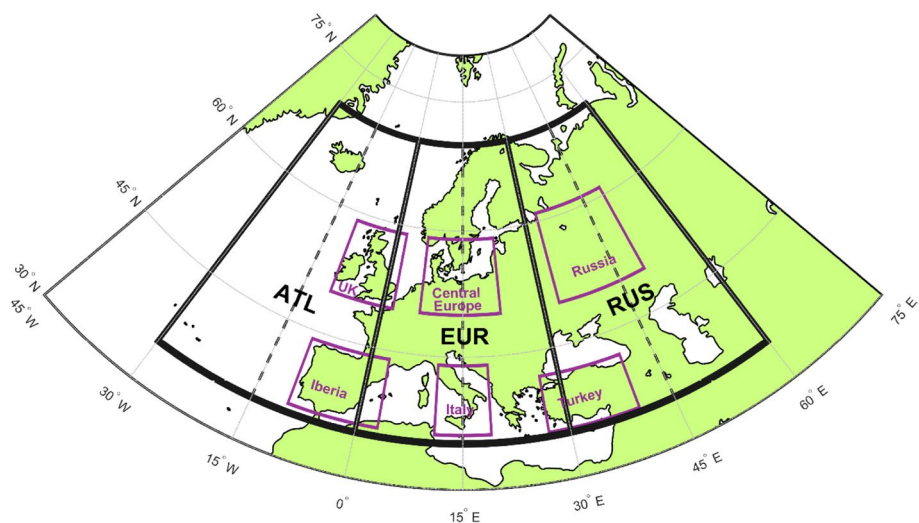
2.2 Blocking and Ridge catalogues

The catalogue of days adopted in this work for high-latitude blocking (hereafter only referred as blocking) was developed by Barriopedro et al. (2006). The algorithm is an adapted version of the Tibaldi and Molteni (1990) index based on the reversal of the meridional Z500 gradient around the typical latitudes of the extra-tropical jet stream.

It further imposes spatial (minimum longitudinal extension of 12.5°) and temporal (minimum duration of 5 days) criteria to account for the characteristic spatio-temporal scales of blocking. The algorithm also enables the characterization of useful daily parameters, such as the location of the blocking center, the intensity or the spatial extension. Following previous studies (Sousa et al. 2015, 2016), where the same catalogue was used to assess the impacts of blocking patterns on precipitation regimes over Europe, three non-overlapping blocking sectors covering the Europe and the eastern Atlantic are defined. More specifically, daily blocking occurrences are assigned to one of the following spatial sectors according to the location of their blocking centers (Fig. 1): ATL (30° – 0° W), EUR (0° – 30° E) and RUS (30° – 60° E).

To compute the catalogue of sub-tropical ridge days (hereafter only referred to as ridges), we follow a similar methodology as in Santos et al. (2009), which is based on daily anomalies of the Z500 field. In order to compare it with the blocking catalogue, we also classified ridge occurrence into the same three sectors (ATL, EUR and RUS). Furthermore, each sector is split into two halves: south (30° – 50° N) and north (50° – 70° N). These latitudinal bands are used for winter and, to accommodate the annual cycle, they are shifted 5° northward for summer. This partition enables classifying ridges as strong Z500 positive departures in sub-tropical and mid-latitudes that do not extend significantly northwards, thus avoiding overlapping days between blocking and ridge patterns. For each grid point, we computed Z500 departures for each specific day, and a 30-day running threshold based on the 80th percentile of the daily Z500 series. We then obtained, on a daily basis and for each longitudinal sector, the percentage of area above that threshold in its northern and southern halves. To classify a ridge day in one of the three considered longitudinal sectors the following criteria are employed: (1)

Fig. 1 Geographical representation of the considered sectors for blocking location (*thick black frames*): Atlantic (ATL)—from 30° W to 0° W; European (EUR)—from 0° to 30° E; Russian (RUS)—from 30° E to 60° E. Each of these sectors was also sub-divided into two smaller 15° longitude-wide sub-sectors (west and east, *dashed black lines*). *Magenta boxes* identify areas for regional-scale assessments (cf. Section 3.4)



at least 75% of the area in the southern half is above the threshold; (2) less than 50% of the area in the northern half is above the same threshold. These percentages and thresholds were tested and calibrated in order to avoid overlaps between blocking and ridge dates, and furthermore to obtain climatological ridge frequencies comparable to previous studies (e.g. Santos et al. 2009).

We also evaluate for each blocking and ridge day the contribution to grid point temperature anomalies of three major physical forcings: horizontal advection, vertical advection and diabatic processes. This is carried out by separating and identifying the process associated with the largest daily temperature change at each grid point (considering only those cells where the absolute temperature anomalies exceed 1 °C under the given weather regime). Daily mean horizontal and vertical temperature advectons are explicitly calculated as in Equations (1) and (2), respectively:

$$\left(\frac{\Delta T}{\Delta t}\right)_h(\lambda, \phi, t) = -\vec{v} \cdot \nabla_p T \quad (1)$$

$$\left(\frac{\Delta T}{\Delta t}\right)_v(\lambda, \phi, t) = -\omega \frac{T}{\theta} \frac{\partial \theta}{\partial p} \quad (2)$$

where the term $\left(\frac{\Delta T}{\Delta t}\right)_h$ is the temperature advection by the horizontal wind, and $\left(\frac{\Delta T}{\Delta t}\right)_v$ the temperature advection

by vertical motion. Equations (1) and (2) are computed from daily mean fields in constant pressure coordinates, according to the pressure levels available in the NCEP/NCAR dataset, with (λ, ϕ, t) representing latitude, longitude and time, respectively, and v being the horizontal wind, T the temperature, ω the vertical velocity and θ the potential temperature. The daily mean temperature rate due to diabatic processes, $\left(\frac{\Delta T}{\Delta t}\right)_d$, is estimated as a residual from the previous two terms based on the temperature tendency equation:

$$\left(\frac{\Delta T}{\Delta t}\right)_d(\lambda, \phi, t) = \frac{\Delta T}{\Delta t} - \left(\frac{\Delta T}{\Delta t}\right)_h - \left(\frac{\Delta T}{\Delta t}\right)_v \quad (3)$$

where $\frac{\Delta T}{\Delta t}$ is the daily mean temperature tendency (in K day⁻¹). The residual approximation for the diabatic term has been previously applied to reanalyses datasets in Chant and Nigam (2009) or Wright and Fueglistaler (2013). It must be kept in mind that different factors such as sub-grid turbulent mixing, analysis increments and other numerical errors may contribute to the residual term. Further, this approach does not consider sub-daily fluctuations of the contributing terms, potential interactions among the underlying processes and feedbacks between the dynamics and thermodynamics. For example, in addition to horizontal warm advection, diabatic and adiabatic heating experienced during the re-circulation of air masses around high pressure systems can contribute to the warm anomalies. Similarly,

warm temperatures induced by a given weather system can in turn modulate the contributing terms by reinforcing the Z500 anomaly. Thus, the attribution of the temperature responses should be taken with caution, as some one-directional causal relationships cannot be fully inferred from a composite analysis.

This bulk analysis is performed for the 1000–850 hPa layer. Then, we compute the daily anomalies of all terms in Eq. (3) and the relative contribution of each term $\left(\frac{\Delta T}{\Delta t}\right)_i$ (in %) to the total change $\left(\frac{\Delta T}{\Delta t}\right)'$, where primes denote daily anomalies. Finally, we derive the composited values of $\left(\frac{\Delta T}{\Delta t}\right)_i$ for blocking and ridge days, and the leading process i with the largest contribution to the temperature tendency anomaly.

In this work, the analyses are performed for winter and summer separately, using the meteorological seasons: December to February and June to August, respectively. The statistical significance of the anomalies presented in the “Results” section was assessed with a two-sample Kolmogorov–Smirnov test (the 5% significance level was considered).

3 Results

3.1 Blocking and ridge seasonal distribution

The classification of events according to their position enables a simple and objective way of grouping blocking and ridge days in each sector and season. It also allows the computation of composites for the aforementioned meteorological variables under each specific synoptic pattern. The winter and summer composites of Z500 anomalies for blocking and ridge days of each sector are shown in Fig. 2. Overall, blocking and ridges display a clear difference in the latitude of their maximum Z500 anomalies. The composites for blocking days show an omega-like structure, which is distinguishable from the non-wave-breaking pattern that is evident in the composites corresponding to days of ridge. Furthermore, the absolute anomalies are larger in winter, and for blocking regimes (Fig. 2a–c). During winter, around one-third of the days comprises blocking occurrence in at least one sector of the Euro-Atlantic region, while summer frequencies are smaller, particularly over the ATL sector (Fig. 2g). The composites accurately capture the signatures associated with blocking over preferred sectors of occurrence in the Eurasian sector (Barriopedro et al. 2006). It is still worth noting that some events contribute to the composites of more than one sector during their lifecycle (Sousa et al.

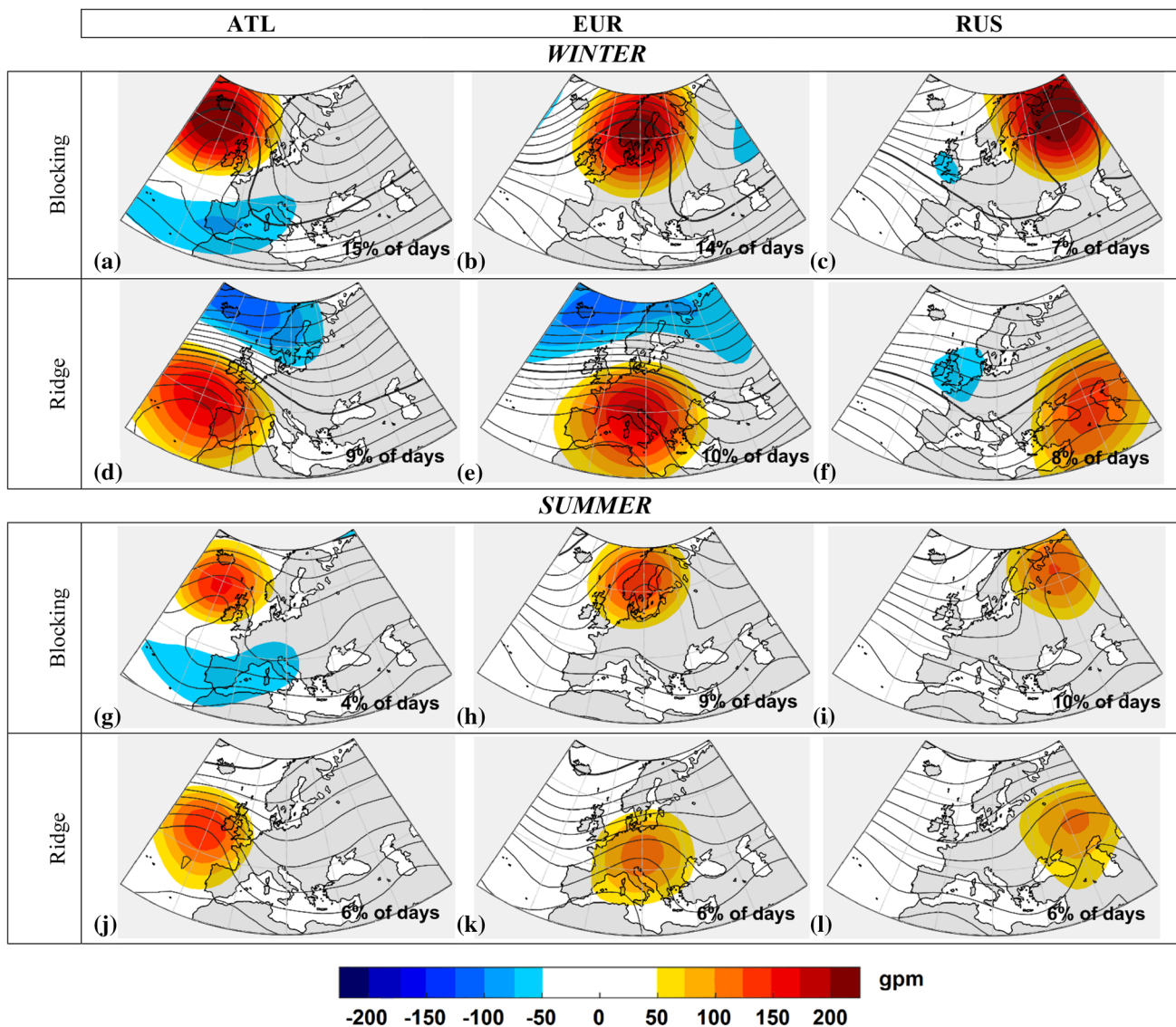


Fig. 2 Composites of the daily anomalies (*shaded areas*) and absolute values (*contours*) of the 500 hPa geopotential height for blocking centers and ridges in each sector, during winter (*upper panels, a–c and d–f, respectively*) and summer (*lower panels, g–i and j–l, respectively*).

All values are in gpm and the thick line represents the 5500 isohypse (the thinner contours are separated by 50 gpm). The seasonal frequencies of occurrence for each regime are shown in percentage.

2016). Ridge frequencies are more equally distributed throughout the three sectors and seasons, with closer values to those of blocking during summer. The largest Z500 anomalies under ridging patterns are found for ATL and EUR ridges in winter (Fig. 2d, e). The positive anomalies of Z500 during blocking and ridge regimes are often accompanied by negative anomalies, but much less pronounced. The most relevant negative Z500 anomalies occur southwards (northwards) of the blocking (ridges) centers, mainly for ATL structures in winter (Fig. 2a, d).

In the following sub-sections, the specific surface temperature responses driven by each weather regime, as well

as the corresponding synoptic environments, will be analyzed in more detail.

3.2 Seasonal temperature responses

Using the seasonal and regional catalogues of blocking and ridge days, we computed the corresponding composites for the maximum and minimum T2m anomalies. In Figs. 3 and 4 we present the maximum (TX) and minimum (TN) temperature anomalies for winter and summer, displaying only statistically significant anomalies at the 5% significance level.

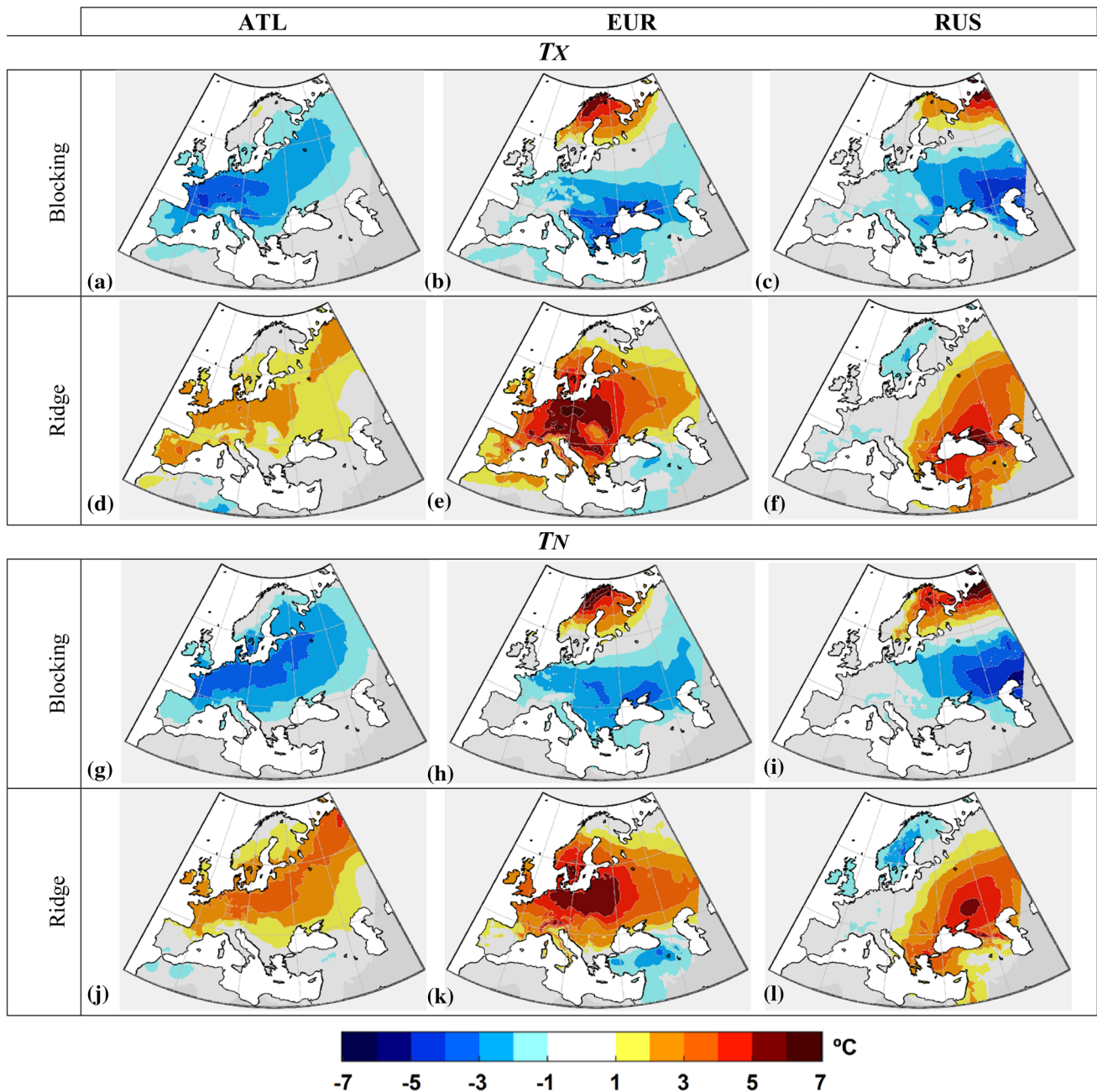


Fig. 3 Composites for blocking and ridge days occurring in each sector (ATL, EUR and RUS) of winter 2 m above ground maximum (upper panels TX; a–c and d–f, respectively) and minimum tempera-

ture (lower panels TN; g–i and j–l, respectively) anomalies (in °C). Only statistically significant anomalies at 5% significance level are depicted

Overall, the geographical locations of the anomaly patterns undergo west-east shifts, in agreement with the positioning of the considered blocking or ridge structure (as presented in Fig. 2). Additionally, there is a clear seasonality in the responses to blocking and ridge patterns, as they typically extend over larger areas in winter than in summer. Furthermore, the temperature responses to blocking are opposite to those of ridges in winter, but not in summer.

These distinctive signatures highlight the need of distinguishing between blocking and ridges, including their spatial scales and location.

The responses in TN and TX are generally coherent for all sectors and regimes during winter (Fig. 3) and reveal highly contrasting patterns between blocking and ridges (Fig. 3a–c versus 3d–f). While during blocking most of Europe experiences well below average temperatures, ridge

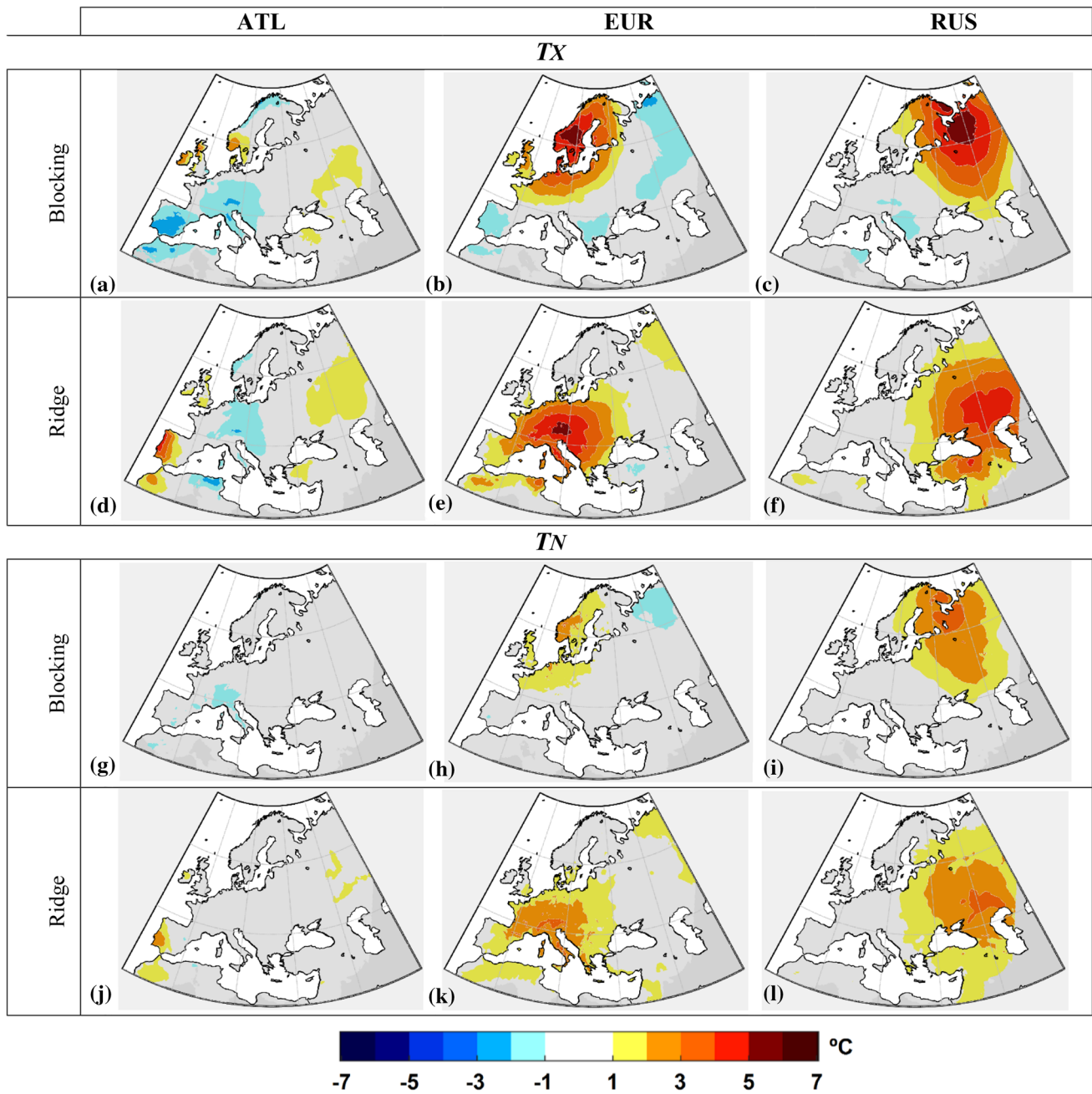


Fig. 4 Same as in Fig. 3, but for summer

days are characterized by extensive above average temperatures. Negative anomalies exceeding -3 °C tend to occur southward and eastward of the blocking centers, with ATL blocking (Fig. 3a) revealing the largest widespread signal over the continent. During blocking episodes, strong positive temperature anomalies are found in land areas under the highest Z500 anomalies (Fig. 2), i.e. northern half of Scandinavia for EUR blocks (Fig. 3b) and northern Russia and eastern Scandinavia for RUS blocks (Fig. 3c). Conversely, winter ridges in both ATL and EUR sectors

(Fig. 3d, e) are responsible for anomalously warm conditions in almost all regions of Europe. These anomalies are particularly striking for EUR ridges (Fig. 3d), when Central Europe experiences positive TX anomalies reaching up to 7 °C. There are some areas on the ridge's eastern and western flanks that experience slightly below average temperatures, mainly in Mediterranean regions. This is particularly noteworthy in Turkey during EUR ridges (Fig. 3k), though these negative anomalies are smaller in magnitude and spatial extension than their positive counterparts.

As previously mentioned, summer temperature anomalies (Fig. 4) are more spatially confined than in winter and the opposite temperature response to blocking and ridge patterns is no longer observed (Fig. 3). In the case of blocking systems, positive anomalies are again centered under the maximum Z500 anomaly area, but now affecting larger areas. In particular, during EUR (RUS) blocking, extensive areas of Central Europe and Scandinavia (Eastern Europe and Russia) experience anomalously warm conditions, with TX anomalies >5 °C, as seen in Fig. 4b, c). Temperature anomalies for ATL blocking (Fig. 4a) are much less pronounced. As in winter, negative anomalies are found in the southern and eastern flanks of blocking systems, but they are small in magnitude, and mostly restricted to TX. Still, southern areas of Europe (e.g., Iberia, Balkans) display negative temperature anomalies associated to blocking in both winter and summer.

Summer ridges are associated with above normal temperatures over a more confined area than in winter. In particular, they do not have significant effects in temperature over northernmost areas of Europe during this season. The lack of opposite signed responses to blocking and ridges during summer is evident in some regions, such as Central Europe or Russia, which experience above average surface temperatures under both regimes, albeit at different latitudes. On the contrary, in southernmost areas, particularly the Iberian Peninsula for ATL regimes (Fig. 4a, d), positive temperature anomalies during ridge days tend to be replaced by negative anomalies during blocking days. Furthermore, summer temperature anomalies over southern Europe critically depend on the specific location of ridge structures.

Although their locations are similar, TX anomalies during summer ridges (Fig. 4d–f) are larger in magnitude than those of TN (Fig. 4j–l). This different amplitude in the daytime and night-time temperature responses is much more pronounced than during winter, which is also observed for blocking systems (Fig. 4a–c vs 4g–i). This is particularly relevant for the occurrence of extremely hot days in summer. In this sense, it is worth noticing that a given synoptic pattern can affect very differently areas situated relatively close, as shown by García-Herrera et al. (2005) when comparing the weather regimes associated with local heatwaves in Lisbon and Madrid. Therefore, a finer-scale analysis using smaller regional sectors is required to address local extreme events. In Figs. S1 and S2 of the Supplementary Material we show the winter and summer composites of TX and TN, considering narrower longitudinal sub-sectors for blocking and ridge location (15° longitude-wide). Overall, the results are similar to those of Figs. 3 and 4, although the temperature responses to summertime ridges are more spatially restricted, especially in western Europe. As an illustration for the Iberian Peninsula, the exact areas

under intense summer hot conditions are very dependent on small west-east shifts in the position of the sub-tropical ridge (Fig. S2g–i). Thus, some regional impacts can be smoothed out in the analysis using larger sectors. However, on the whole, the analysis based on three 30° longitudinal sectors is sufficient to identify the most relevant temperature responses to blocking and ridges, as well as the associated mechanisms, which are described in the following section.

3.3 Synoptic and forcing mechanisms

In this section we apply the methodology described in Sect. 2 in order to assess the relative contribution of different processes to the local temperature anomalies associated with blocks and ridges, namely: (1) horizontal advection by the large-scale flow; (2) vertical advection–adiabatic heating/cooling; (3) diabatic processes. In most cases one dominant mechanism can be identified, though local temperature responses can also be due to a combination of the forcing terms, frequently involving a partial cancelation in the net temperature tendency. For the sake of succinctness, only the leading term is shown in Fig. 5, and the full analysis of the heating/cooling fraction due to each specific term is presented in the Supplementary Material (Figs. S3 and S4).

During winter (Fig. 5a–c) and summer (Fig. 5g–i) blocking days, horizontal advection by anomalous southerly flows appears responsible for a large fraction of the warming observed in the northwestern flank of the blocking systems, with the exception of winter RUS blocks. The negative temperature anomalies found in the southeastern flank of the blocking center, particularly striking during winter, are also predominantly a result of cold advection from higher latitudes under the northerly flow established along the eastern flank of the high-pressure system (see the anomalous wind fields in Fig. 5a–c). This colder air is carried towards southern Europe (e.g. north of the Black Sea), thus interacting with different air masses. As a result, other processes, such as diabatic cooling, and in particular, convective processes in warm seasons, can gain further importance in localized areas to the southeast of the blocking centers (Sousa et al. 2016). This mixed contribution of different forcing terms at lower latitudes under blocking occurrence is confirmed by Fig. S3 and S4. In areas under the maximum geopotential height anomaly, warming due to reinforced subsidence and diabatic heating gains particular relevance, particularly for continental blocks. There are also differences in the relative contribution of each term depending on the season (Fig. 5a–c, g–i): warming due to horizontal advection is relevant during both winter and summer blocks, while anomalous downward motion is mostly relevant for winter blocking. On the other hand,

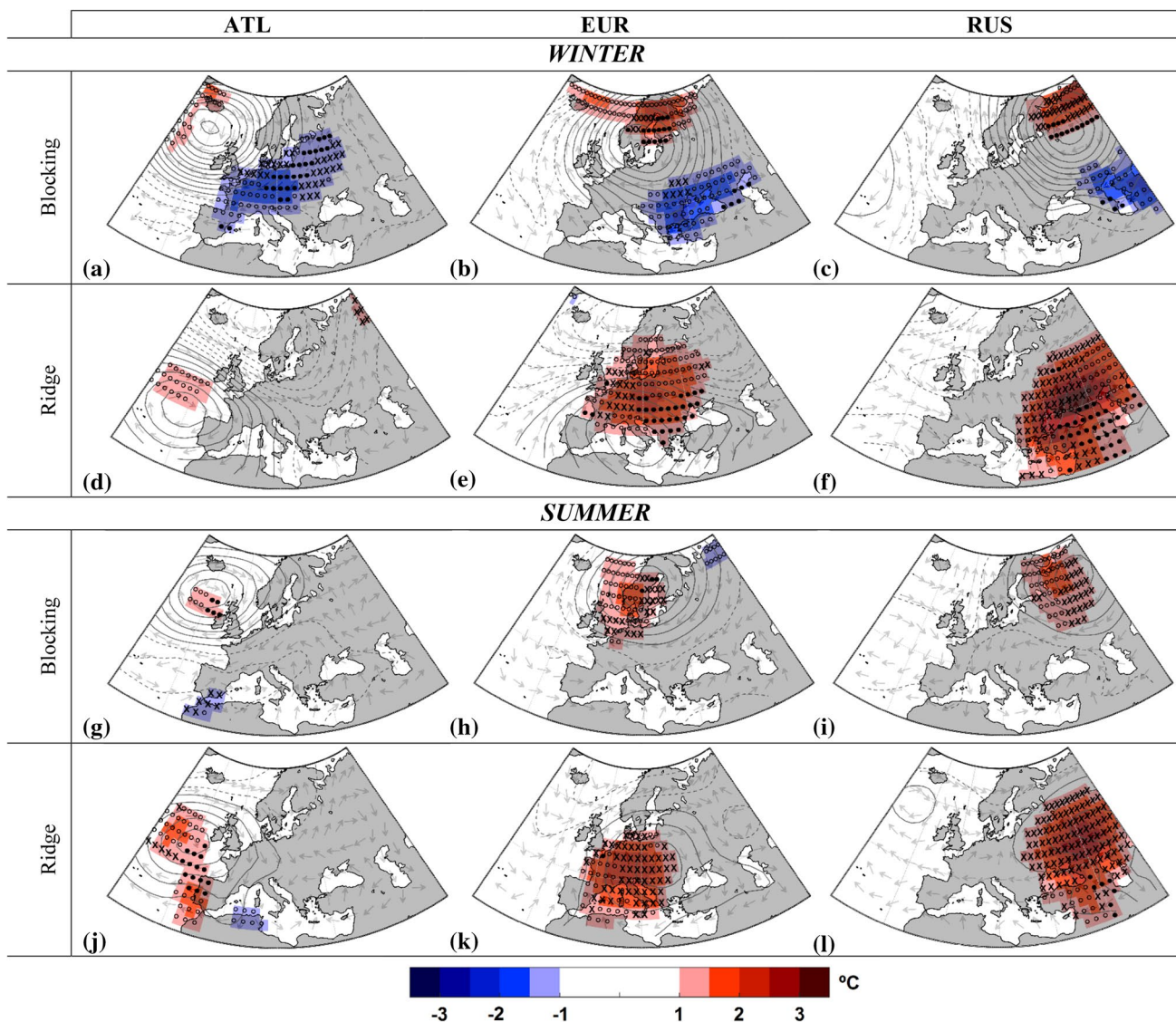


Fig. 5 Mechanisms related to temperature anomalies in the lower troposphere (1000–850 hPa) during blocking and ridge days during winter (*upper panels, a–c and d–f, respectively*) and summer (*lower panels, g–i and j–l, respectively*). *Color shadings* depict anomalies in the mean daily temperature (in °C). *Solid (dashed) contours* represent

positive (negative) 500 hPa geopotential height anomalies in 15 dam intervals. *Light grey vectors* show anomalies in the horizontal wind direction. *Symbols* denote the highest contributing mechanism for the observed temperature changes at each grid point: horizontal advection (O), vertical advection (●) and diabatic processes (X)

significant diabatic heating dominates in summer, predominantly over continental areas (Fig. 5h, i). As shown later, the summer dominance of the diabatic term over land areas is well explained by changes in the radiative flux budgets.

Regarding ridge days, warm horizontal advection from Atlantic air masses influences the temperature responses in the northern flank of the ridge, particularly during winter ATL and EUR ridges (Fig. 5d, e). This is associated with the passage of cyclones, but also with the corresponding changes in cloud cover and long-wave fluxes,

as explained below. Similarly to blocking, subsidence and diabatic processes are crucial in continental areas under the influence of winter and summer sub-tropical ridges (Fig. S3m-r and S4m-r). Adiabatic heating due to strong subsidence extends over larger areas in winter than in summer, mostly eastwards of the maximum Z500 anomalies (Fig. 5e, f), while diabatic heating dominates the summer temperature responses (Fig. 5k, l). Over the Iberian Peninsula, subsidence and horizontal advection towards southwestern coasts are the main driver for above average summer temperatures during ATL ridges.

It should be stressed that NCEP/NCAR temperature anomalies for the considered layer do not fully overlap with the TX and TN anomalies of the E-OBS datasets in all areas and for all regimes, thus partially explaining some discrepancies between the areas highlighted in Figs. 5, 3 and 4. Still, there are also some important dynamical features related to these discrepancies. For example, negative T2m anomalies during winter blocking (Fig. 3a–c, g–i) are more widespread than aloft (Fig. 5a–c). In particular, some areas with negative near-surface temperature anomalies display simultaneously positive anomalies in the highest level of the considered layer (850 hPa, not shown). This indicates a typical pattern of thermal inversion under high pressure systems, which extends westwards of the blocking center (see Fig. S5a–c). The thermal inversion and the corresponding imprisonment of cold air at lower levels are typical of enhanced long-wave radiative cooling, thus stressing the importance of diabatic processes for the near-surface temperature responses. During summer, the well-mixed boundary layer determines a better agreement between anomalies at surface and aloft, supporting the smaller role of horizontal advection when compared to other processes, particularly those associated to diabatic heating.

Up to now, we have shown that diabatic processes are key to determine the near-surface temperature responses to blocking and ridges, particularly in summer. The diabatic term includes different processes, such as radiative fluxes, latent and sensible heat fluxes and frictional dissipation. To better frame the observed temperature responses to the weather regimes and the seasonal-dependent role of the diabatic term, we computed composites of surface radiative fluxes for blocking and ridges in winter (Fig. 6) and summer (Fig. 7), along with composites of total cloud cover anomalies (Fig. 8).

The radiative forcing over Europe during winter blocking episodes is not remarkable, at least concerning short-wave fluxes (Fig. 6d–f), which are quite modest in high latitudes during months with reduced insolation. Anomalies are rather dominated by the gains (losses) in surface net long-wave fluxes, which in turn are strongly associated with above (below) average cloud cover (see also Fig. 8a–c). For example, near the blocking centers, the enhanced nocturnal long-wave losses (Fig. 6a–c) under clear sky conditions are partly offset by diurnal short-wave gains (Fig. 6d–f). This winter radiative surface cooling signal is in agreement with that in the 1000–850 hPa layer due to the diabatic term (Fig. S3g–i), which is the leading process in areas to the southeast of the ATL and EUR blocking centers (Fig. 5a, b).

The radiative fluxes anomalies during winter ridges reveal an increase in diurnal radiative heating near the Z500 maximum (Fig. 6m–o), due to positive net short-wave fluxes under enhanced clear sky conditions over

Iberia (ATL), Balkans (EUR) and Middle East (RUS). However, this signal is offset by the opposite negative long-wave fluxes (Fig. 6j–l) over the same southern regions, as reflected in the total radiative budget (Fig. 6p–r). In contrast, areas north of the ridge structures exhibit significant increases in cloud cover (Fig. 8d–f), which lead to positive anomalies in the surface long-wave (Fig. 6j–l) and total (Fig. 6p–r) radiative budgets. A similar increase in long-wave and total radiative fluxes is found north of the blocking systems, but restricted to very high latitudes (Fig. 6a–c, g–i). The winter radiative heating is particularly relevant for the UK and coastal areas of central Europe under ATL or EUR ridges (Fig. 6j, k), as well as some Mediterranean areas during EUR and RUS ridges (Fig. 6k, l). Its combined effect with the advection of mild Atlantic air masses explains the large positive near-surface temperature responses during ridge days (Fig. 3d–f). However, as long-wave radiative fluxes tend to cancel out the short-wave fluxes, on the overall diabatic processes are less important in the 1000–850 hPa layer than subsidence or advection, with the exception made for northern Russia (Fig. 5d–f).

During summer, anomalies in radiative fluxes are larger than in winter, in accordance with the stronger contribution from diabatic processes (Fig. 5g–l) and an increase in insolation hours. Like in winter, below average cloud cover (Fig. 8g–l) over the centers' systems results in simultaneous warming by diurnal radiative gains (Fig. 7d–f, m–o) and cooling by nocturnal radiative losses (Fig. 7a–c, j–l). Nonetheless, and different to winter, the summer increases in short-wave income are stronger in magnitude than the enhanced nocturnal surface long-wave losses over areas under the blocking and ridges centers. Thus, short-wave gains clearly dominate in summer, and the resulting net radiative balance (Fig. 7g–i, p–r) explains well the larger anomalies for TX than for TN. The subsequent increase in daily temperature range can be found for both blocking and ridge regimes, being particularly remarkable at higher latitudes for blocking episodes, and also for central Mediterranean areas during EUR ridges. On the other hand, areas south of blocking and north of ridges experience losses in net short-wave fluxes and gains in long-wave radiation. This is in agreement with increases in cloud cover (Fig. 8g–l) due to the deflection of humid Atlantic westerly flows around the high pressure centers (e.g., Trigo et al. 2004; Sousa et al. 2016). This effect on the radiative budget due to increased cloudiness is particularly evident for Atlantic areas in summer, when comparing ATL ridges to those located in EUR or RUS (Fig. 7p–r).

Note that the local temperature changes that were attributed essentially to diabatic processes (Fig. 5) do not always reflect heating/cooling strictly due to anomalous surface radiative fluxes (Figs. 6, 7). Sensible and latent heat fluxes are very important to transfer these

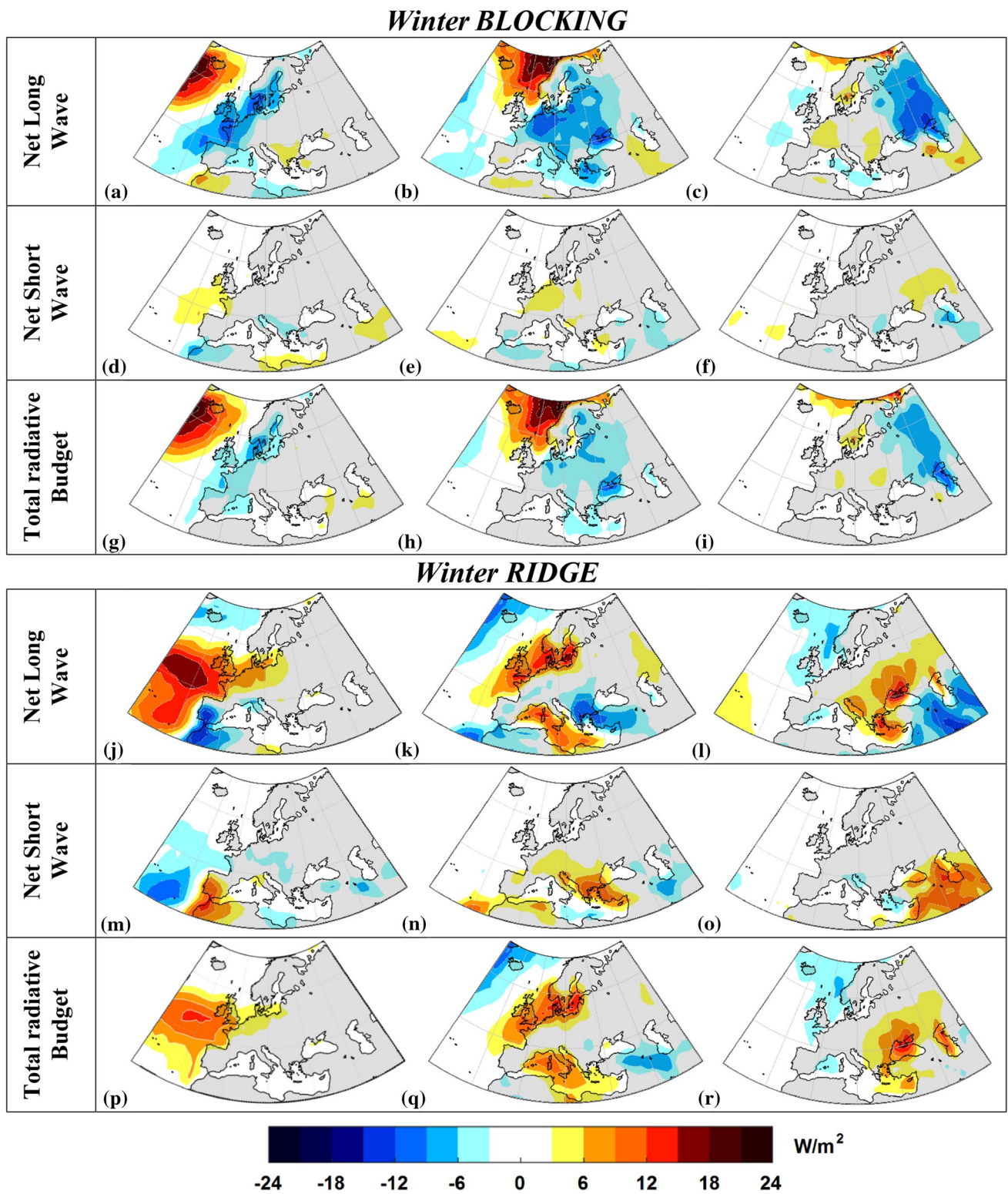


Fig. 6 Composites of net surface longwave and shortwave radiative flux anomalies and corresponding total radiative budget ($W\ m^{-2}$) for blocking (*upper panel; a–c, d–f and g–i, respectively*) and ridge

(*lower panel; j–l, m–o and p–r, respectively*) days during winter. Reddish (bluish) colors correspond to positive (negative) fluxes towards the surface

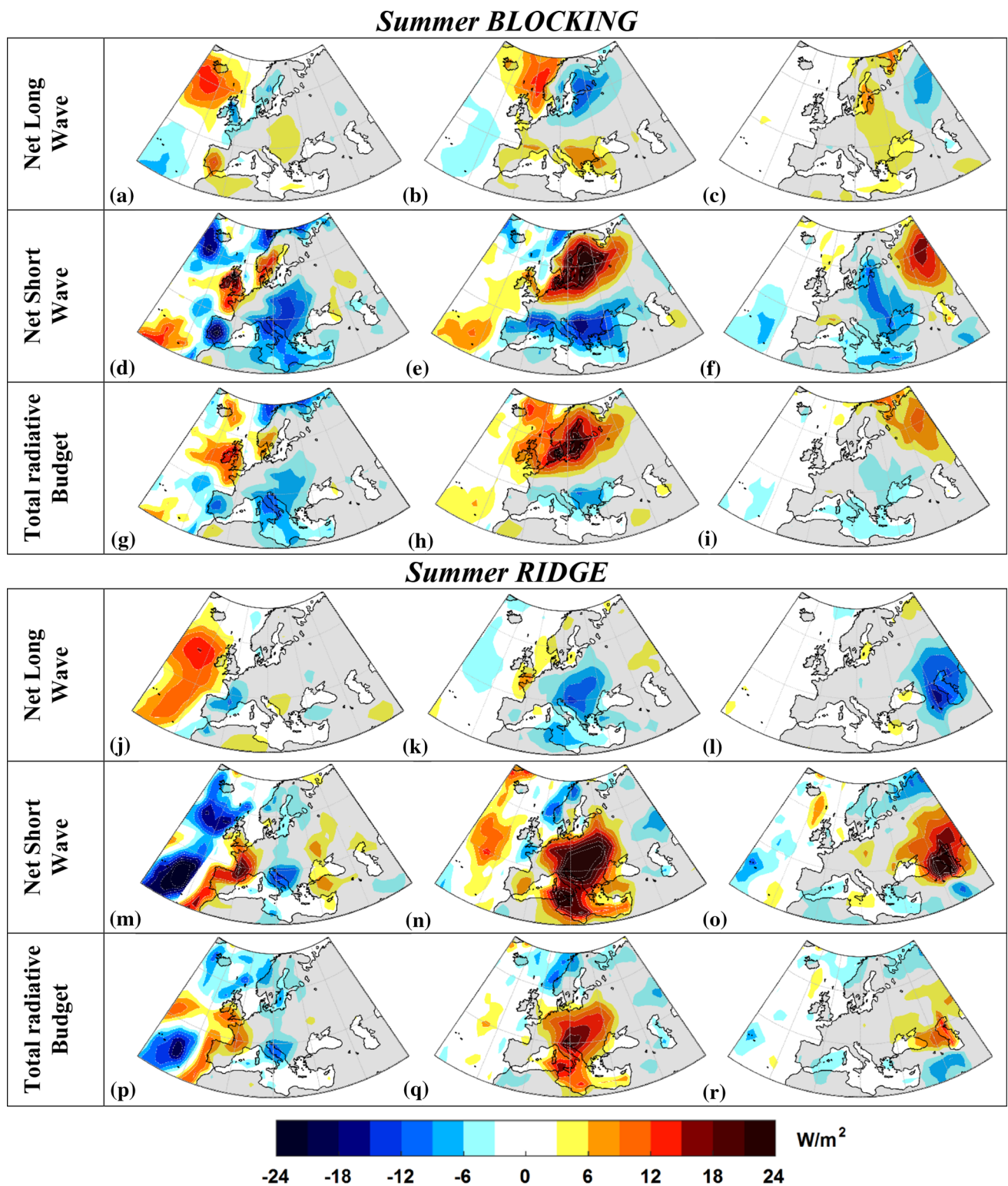


Fig. 7 Same as Fig. 6, but during summer

surface anomalies to the atmosphere. In addition, warming owed to friction can also be relevant on the overall diabatic term, particularly during winter. We

acknowledge the relevance of a deeper assessment of such terms but a full analysis is out of the scope of the present work.

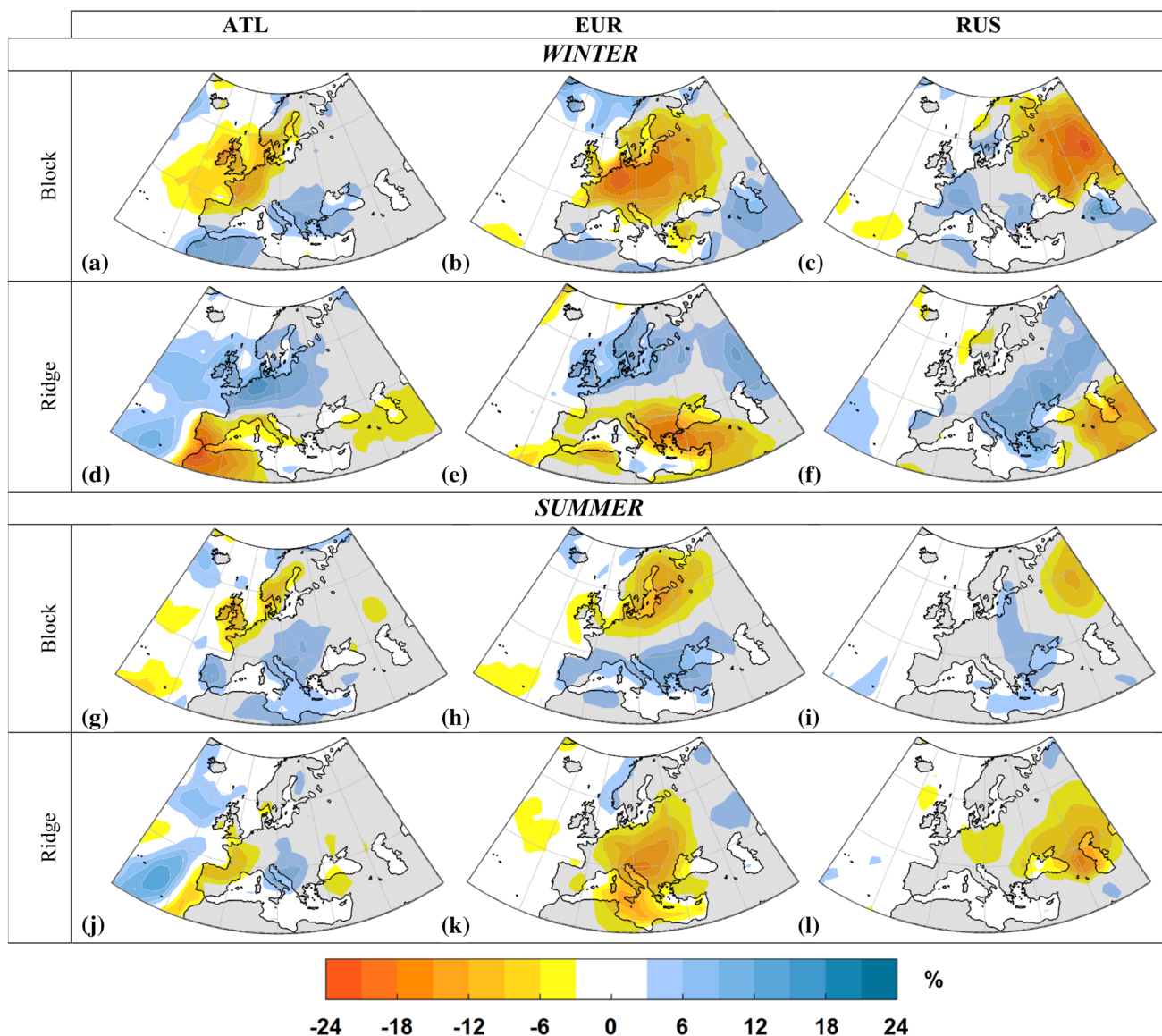


Fig. 8 Composites of the total cloud cover anomalies (%) for blocking and ridge days occurring in each sector during winter (*upper panel*; **a–c** and **d–f**, respectively) and summer (*lower panel*; **g–i** and **j–l**, respectively)

3.4 Changes in regional temperature distribution

In this section we will analyze regional changes in the Probability Density Function (PDF) of daily TX and TN for each weather regime. These regional temperature responses will also be related to the previously discussed forcing mechanisms. The PDF analysis was performed using all grid point series of each region highlighted in magenta in Fig. 1. We computed regional PDFs for all days of each season and for each regime separately (Figs. 9, 10), along with the corresponding changes in mean TN and TX and in their temporal variance. We also measured the degree of homogeneity inside each region (σ_T), by computing the standard deviation of the mean local temperatures of all

grid points, thus accounting for the dispersion of the climatological TX and TN values within each region. As it can be seen in Figs. 9 and 10 the regions with larger values of σ_T comprise important orographic barriers (Iberia, Italy and Turkey).

Figure 9 indicates that wintertime PDF temperature distributions over the considered regions are generally shifted towards lower values for blocking, and higher values for ridge patterns. Warming due to the presence of ridge structures is on the overall larger than cooling due to blocking. The anomalous warming driven by winter ridges may lead to high temperatures over large parts of Europe, such as the Central European region (Fig. 9e, f). For this region, EUR ridges (red dashed lines in Fig. 9)

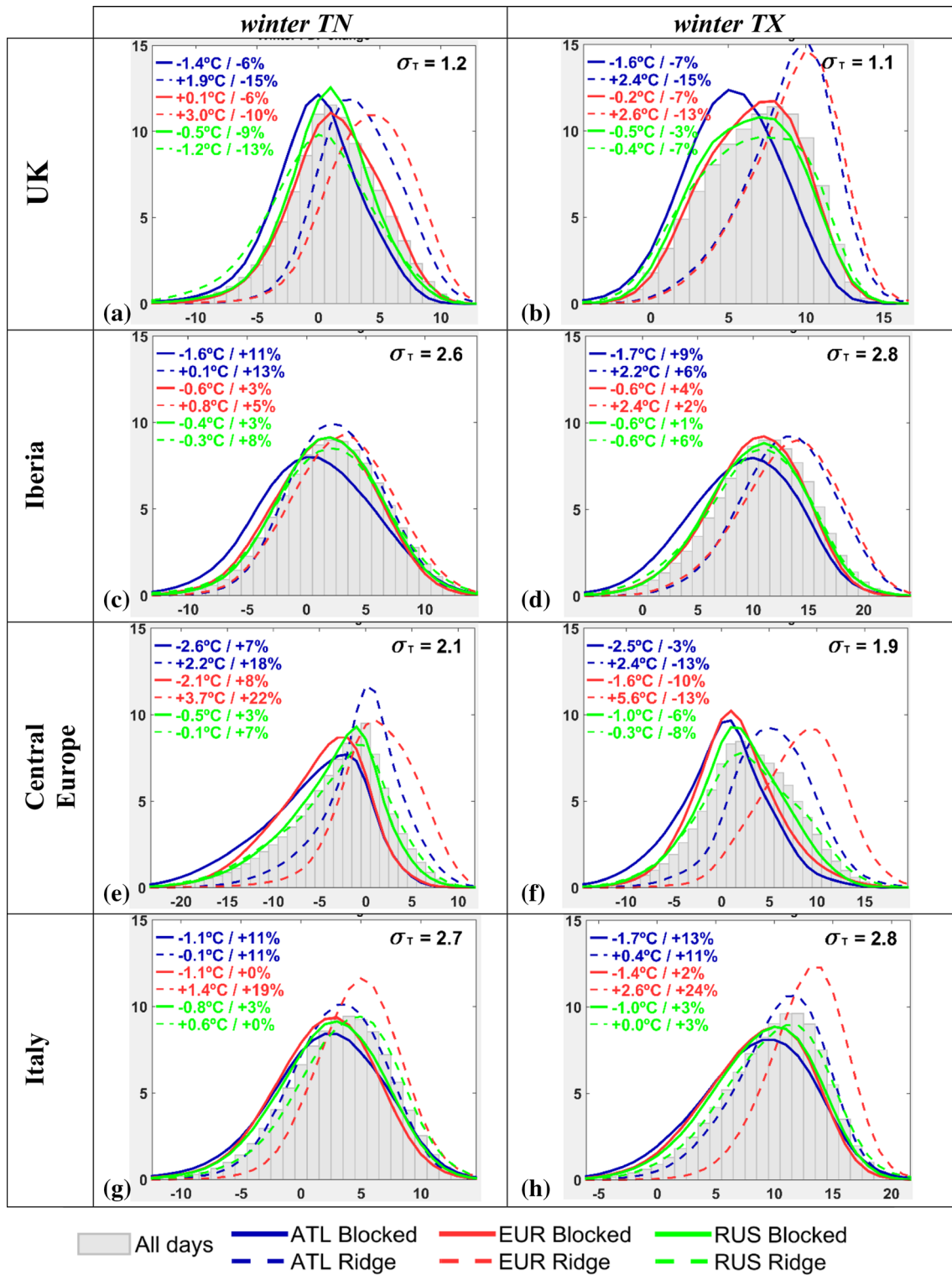


Fig. 9 Distributions for winter minimum (left panels TN) and maximum (right panels TX) 2 m above ground temperature frequency (%) for blocking and ridge days and for the four regional sectors depicted in magenta in Fig. 1 [UK (a, b); Iberia (c, d); Central Europe (e, f) and Italy (g, h)]. Grey bars denote seasonal climatology, solid lines

correspond to blocking days and dashed lines to ridge days. Upper left values represent the corresponding changes in mean temperature ($^{\circ}\text{C}$) and variance (%) with respect to the full distribution parameters, while σ_T shows standard deviations of area-mean temperatures

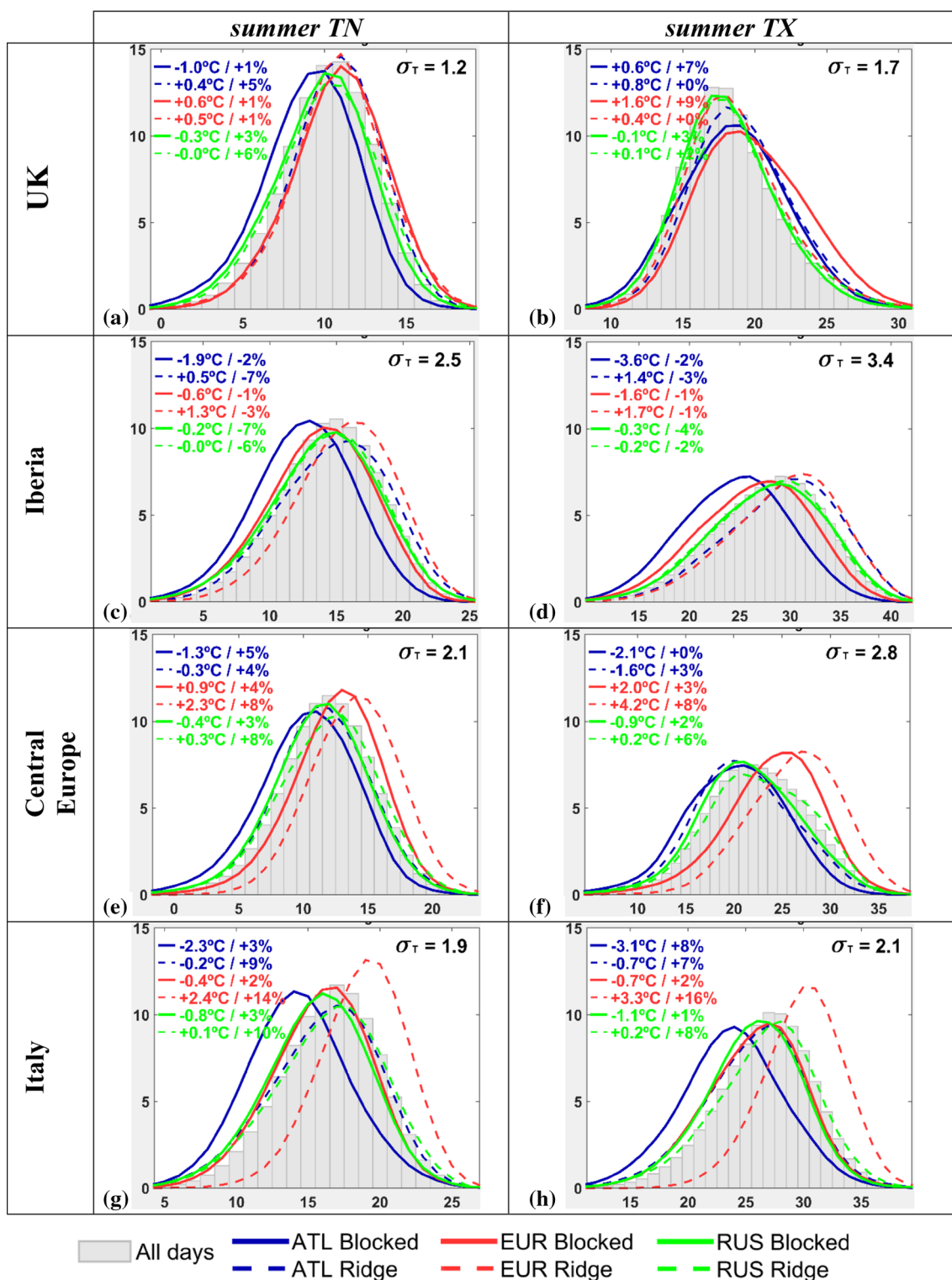


Fig. 10 Same as Fig. 9, but for summer

result in a mean increase in TX of almost 6 °C, and of about 4 °C in TN, as well as abnormally high frequencies of extremely warm winter days, while nights with TN below -10 °C are almost nonexistent. In the UK, the

frequency of days with TX below freezing during ATL (blue dashed lines) and EUR ridge patterns becomes almost negligible (Fig. 9b). While ATL and EUR ridges result in well above average temperatures over most of

Europe, the same is not true for RUS ridges (green dashed lines, Fig. 9). In this case, well above average temperatures are restricted to the easternmost areas of Europe (cf. Fig. S6a-d for Russia and Turkey). However, in areas distant enough to the west of such structures (e.g., UK and Iberia) slightly negative temperature anomalies are found due to the presence of a trough westwards of the RUS ridge (Fig. 2f).

During winter blocking, there is a shift towards colder TX and TN in all regions, which is particularly pronounced for ATL and EUR blocks (blue and red solid lines, Fig. 9). Furthermore, blocking promotes wintertime extreme cold days and nights over large parts of Europe, as inferred from the regional shifts towards the left end tails of the PDF distributions. In particular, ATL blocks are the main drivers of cold days in all regions, since the location of the high pressure center favors cold advection over large areas of the continent (as previously shown in Fig. 5a). For the same reason, during EUR blocks, colder than average temperatures are observed in Central Europe (Fig. 9e, f) and Italy (Fig. 9g, h), extending towards Russia and Turkey (Fig. S6a-d). Remarkable PDF changes during winter RUS blocking are mostly restricted to the easternmost areas, as it was found for RUS ridges.

Winter ridges in the ATL and EUR sectors reduce the variance of TX and TN in the UK (Fig. 9a, b) by more than 10%, while in Central Europe they are associated with smaller (larger) variability in TX (TN), as shown in Fig. 9e (f). On the overall, winter blocking patterns result in qualitatively similar, but smaller changes in variance. For southern sectors, most weather regimes concur with larger wintertime variance in TX and TN. This is particularly clear for the Italian sector (Fig. 9g, h), where TX displays around 25% more variability during EUR ridges.

During summer (Fig. 10), the regional PDF responses to blocking and ridges are no longer opposite in sign for all regions. While ridges (blocks) are still associated with warmer (colder) than average temperatures in the southernmost regions (Fig. 10c, d, g, h), both regimes cause shifts towards higher temperatures in the northernmost regions (Figs. 10a, b, e, f). Larger PDF changes are observed for ridges than for blocks, and in TX than in TN, in agreement with Fig. 4 and the dominant role of short-wave over long-wave radiative fluxes in summer (Fig. 7). In the Iberian Peninsula, there is a very clear rise in the number of days with TX above 35 °C for ATL and EUR ridges when compared to other regimes (Fig. 10d). In Central Europe, EUR blocking and ridge patterns result in an impressive increase in the frequency of days above 30 and 35 °C (Fig. 10f), respectively. As we move to eastern Europe, the RUS patterns become more relevant (see PDF changes for Russia and Turkey in Fig. S6). Concerning summer changes in variance, we found a slight increase for almost all patterns

and regions, particularly pronounced in Italy (Fig. 10g, h) during EUR ridges.

Changes in extreme temperatures associated with blocking and ridges were also investigated for each region of Fig. 1. To do so, we computed for each grid point the number of days below the 10th percentile of winter TN (TN10, hereafter) and above the 90th percentile of summer TX (TX90, hereafter). The percentiles, which were derived from all seasonal days of the period 1950–2012, the occurrence of exceedances and their changes during blocking and ridges were spatially averaged for all grid points of each region. The relative changes in these extreme indices associated with each weather regime are presented in Fig. 11 (expressed in % with respect to that expected from the full 1950–2012 climatology).

Changes in TN10 confirm the previously described opposite responses for blocking and ridge patterns during winter. On the overall, there is an increase in cold winter extremes during blocking (filled triangle symbols in Fig. 10). In particular, the increases in TN10 exceed 10% over Iberia (Fig. 11c) and Central Europe (Fig. 11b) during ATL blocks. On the other hand, ridges (open triangle symbols), especially those occurring in the ATL and EUR sectors, reduce the occurrence of winter cold extremes in all regions. Similar responses to blocking and ridges are found in winter TN10 for easternmost areas (cf. Fig. S7 for Russia and Turkey), but being the RUS patterns more relevant here.

During summer, blocking (filled circles) and ridges (open circles) cause opposite changes in the frequency of extremely hot days in southern Europe (Iberia and Italy, Fig. 11c, d). However, in areas further north (UK and Central Europe, Fig. 11a, b), both weather regimes promote substantial increases in TX90. Thus, while ridging is associated to a rise in the frequency of extremely hot days in almost all regions, the same is not true for blocks, which decrease (increase) TX90 in southern (northern) regions. In particular, nearly 30% more extremely hot days occur in Central Europe and Italy under EUR ridges (Fig. 11b, d, respectively), while in Iberia TX90 increases by around 10% during ATL and EUR ridges (Fig. 11b). Differently, the most important regimes for the occurrence of hot days in the UK are ATL and EUR blocks (Fig. 11a), which cause TX90 increases of around 10% and 15%, respectively. Again, for easternmost areas, weather regimes centered in the RUS sector trigger the largest changes in TX90. Thus, in Turkey (Fig. S7b), extremely hot conditions are driven essentially by RUS ridges, whereas in Russia (Fig. S7a) both RUS ridges and blocks result in a 15–20% increase in TX90. In fact, the impact of anomalous Z500 fields in the Russian area has been widely discussed due to recent events, such as the 2010 Russian mega-heatwave (e.g., Barriopedro et al. 2011).

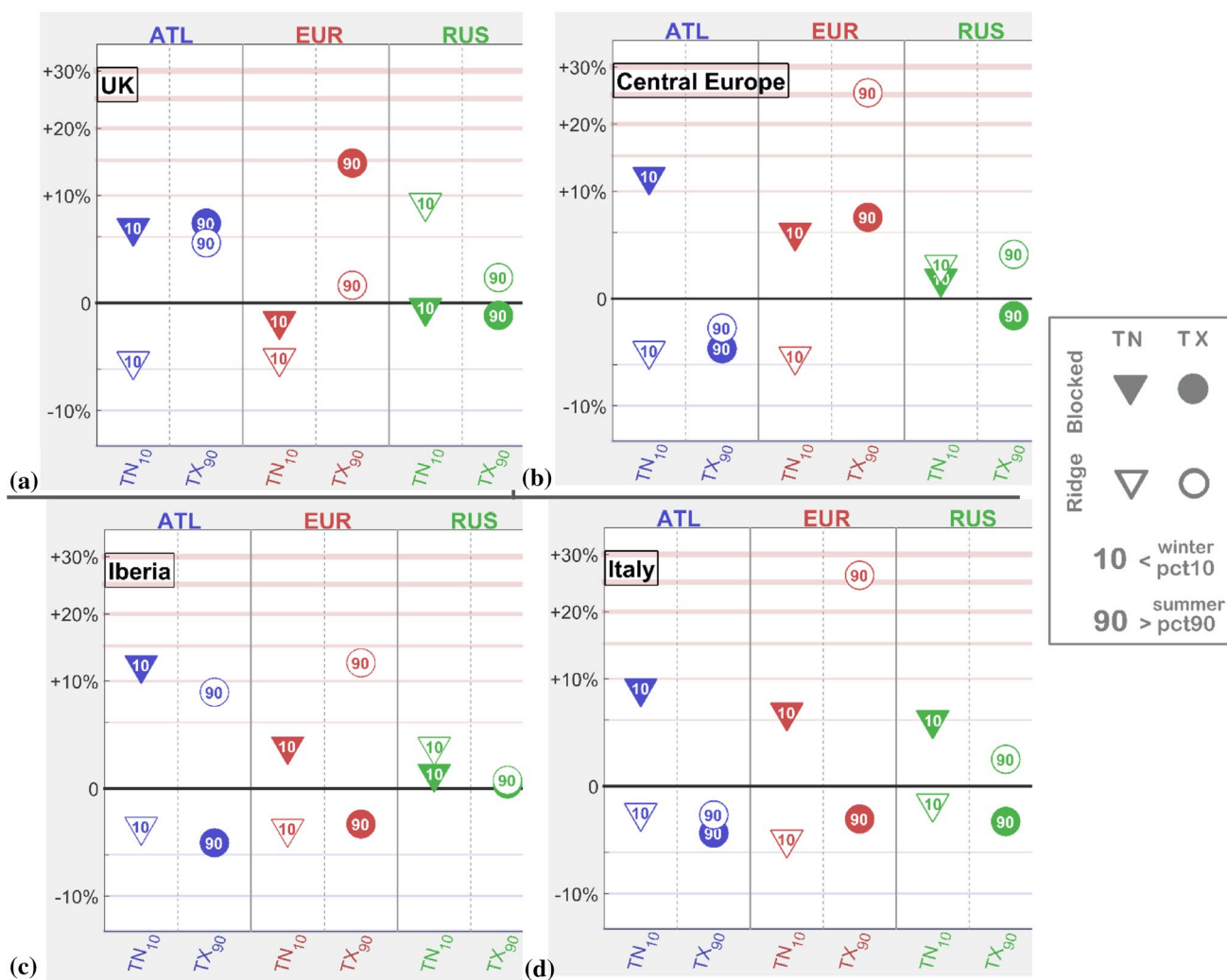


Fig. 11 Relative changes (%) in the frequencies of extreme temperature during blocking and ridge patterns in the regional sectors presented in Fig. 1 [UK (a), Iberia (b), Central Europe (c) and Italy (d)],

using the winter TN10 and summer TX90 indices. Circles (triangles) represent maximum (minimum) temperature, and filled (open) symbols represent blocking (ridge) patterns

4 Discussion and conclusions

In this work we introduced a clear separation between high-latitude blocking structures and sub-tropical ridges occurring in different sectors of the Euro-Atlantic area (30 °W–60 °E), both in terms of climatology and seasonal impacts on temperature in the European continent. While winter blocking characteristics have been extensively studied, our work also focuses on the characterization of blocking impacts on European summer temperature, which has been much less investigated. Furthermore, the extension of this comprehensive analysis towards the sub-tropical ridge phenomenology is a significant novelty. In this sense, this systematical separation between high- and low-latitude structures may be used in other climatological and dynamical applications, besides the one presented in this work.

We introduced an objective separation of the different forcing mechanisms behind the temperature responses associated to each considered weather regime. This approach enabled quantifying the importance of the following forcing factors: horizontal advection, vertical advection and diabatic heating. Particular attention was devoted to the radiative contribution to the diabatic term. To our knowledge, this systematic quantification of the different contributing factors to the temperature responses represents an innovation in the literature of climatological impacts related to blocking and ridge phenomenology—Seo et al. (2016) used a similar approach to link temperature anomalies with the Madden-Julian Oscillation. Despite the limitations in the methodology, the results are in agreement with previous studies which have analyzed air parcel trajectories over Europe and the associated surface temperature responses for some specific case studies or regional weather systems.

Thus, our approach corroborates these results from another perspective, and also distinguishes between the physical mechanisms associated with blocking and ridges, and to what extent they critically depend on their exact locations.

Finally, we complemented our analysis by evaluating changes in the PDF distributions of seasonal maximum and minimum temperature for different European regions, and in the frequency of extremely cold nights in winter and hot days in summer. This assessment allowed a finer look at regional impacts, framing smaller scale responses into the previous larger scale analysis. The main results of this study can be summarized as follows:

- 1 In winter, the synoptic signatures and near-surface temperature responses are generally opposite between blocking and ridge patterns. In particular, most of Europe experiences colder (warmer) than average winter conditions during blocking (ridge) days. On the contrary, the summer temperature responses to blocking and ridges are more regional and not so dissimilar, with above average regional temperatures for both patterns. Negative temperature anomalies are essentially restricted to southern Europe during blocking episodes. The spring transition in the blocking signatures from winter cold to summer warm anomalies in central and northern areas of Europe has been noted recently by Brunner et al. (2017).
- 2 Concerning the regional classification of blocking and ridges, the largest impacts associated to the weather regimes of each specific sector follow the specific longitudinal locations of the maximum 500 hPa geopotential height anomalies. Nevertheless, blocking and ridge structures located over central and western Europe are usually the ones with larger and more extensive temperature anomalies, as they cause the largest disruption of the Atlantic jet stream.
- 3 During winter, the horizontal advection by the anomalous flow plays a dominant role in shaping the lower-tropospheric temperature responses to blocking and ridge systems. In particular, the cold advection of high-latitude air masses towards central and southern Europe during blocking episodes and the transport of Atlantic moist and warm air towards the continent during subtropical ridges are key processes. Over continental areas, long-wave radiative losses associated to blocking and ridges tend to offset the near-surface temperature anomalies induced by changes in short-wave radiation fluxes. In summer, diabatic heating is the most important factor in determining warm temperature anomalies during blocking and ridge regimes. Different to winter, the induced anomalies in short-wave radiative fluxes overwhelm those in long-wave radiative fluxes due to the summer increase in insolation hours. As a consequence, blocking and ridges prompt larger responses in maximum than in minimum temperatures, and a resulting increase in the temperature daily range. The adiabatic heating triggered by reinforced subsidence during blocking and ridges plays a secondary role in rising lower-tropospheric temperatures, being more relevant during winter, and particularly important near the central locations of the anticyclonic circulation.
- 4 This process-oriented attribution has enabled more detailed regional and seasonal analyses, additionally reporting some smaller-scale exceptions. However, some limitations must be acknowledged. For example, although a dominant forcing factor has often been identified, in some cases there is a similar contribution or a partial cancelation between the considered forcings. In spite of this, our results are in agreement with Lagrangian-based studies (Pfahl et al. 2015; Bieli et al. 2015; Santos et al. 2015), which have noticed that winter cold events are associated to long air mass trajectories, whereas summer events are more related to in situ warming due to enhanced radiation and surface heat fluxes.
- 5 On the overall, winter changes in extremely cold temperatures are spatially coherent, with generalized increases (decreases) in the frequency of TN10 during blocking (ridge) occurrence. Summer changes in extremely hot days are more regionally focused during blocking and ridge regimes. This is particularly evident in southern Europe, where we show a clear dissociation between the impacts of blocking (decreases in TX90) and ridges (increases in TX90). Further, the impact of ridges is particularly dependent on the exact longitudinal location of northwards extensions of the sub-tropical ridge belt.

In summary, we have clarified the very distinct role of blocking and ridges in European temperature. This gains particular relevance for summer extreme temperatures in southern Europe, which has been affected by major heatwaves such as the episodes of 2003 and 2007 and is bound to suffer even more frequent heatwaves in coming decades

(Christensen et al. 2013). In this sense, there has been some misperception and imprecise attribution of heat episodes in these areas to classical blocking definitions (e.g. Trigo et al. 2005). We are confident to have achieved a more complete and consistent phenomenological description of the distinctive impacts of blocking and ridges on European winter and summer temperature. Finally, we must acknowledge the relevance of performing further sensitivity analyses using different reanalyses datasets when carrying out specific methodologies as the one performed in this work, namely the temperature tendency diagnostic.

Acknowledgements Pedro M. Sousa was supported by the Portuguese Science Foundation (FCT) through a doctoral Grant (SFRH/BD/84395/2012). Pedro M.M. Soares thanks the Portuguese Science Foundation (FCT) for funding under Project SOLAR-PTDC/GEOMET/7078/2014. This work was also supported by FEDER/COMPETE/POCI—Operational Competitiveness and Internationalization Programme, under Project POCI-01-0145-FEDER-006958 and by FCT-Portuguese Foundation for Science and Technology, under the project UID/AGR/04033/2013. We acknowledge the E-OBS dataset from the EU-FP6 project ENSEMBLES (<http://ensembles-eu.metoffice.com>) and the data providers in the ECA&D project (<http://www.ecad.eu>).

References

- Altenhoff AM, Martius O, Croci-Maspoli M, Schwiers C, Davies HC (2008) Linkage of atmospheric blocks and synoptic-scale Rossby waves: a climatological analysis. *Tellus Series A-Dyn Meteorol Oceanogr* 60(5):1053–1063. doi:10.1111/j.1600-0870.2008.00354.x
- Andrade C, Leite SM, Santos JA (2012) Temperature extremes. Europe: overview of their driving atmospheric patterns. *Nat Hazards Earth Syst Sci* 12:1671–1691. doi:10.5194/nhess-12-1671-2012
- Barriopedro D, Calvo N (2014) On the relationship between ENSO, stratospheric sudden warmings, and blocking. *J Climate* 27(12):4704–4720. doi:10.1175/JCLI-D-13-00770.1
- Barriopedro D, García-Herrera R, Lupo AR, Hernández E (2006) Acclimatology of northern hemisphere blocking. *J Clim* 19:1042–1063. doi:10.1175/JCLI3678.1
- Barriopedro D, García-Herrera R, Trigo RM (2010) Application of blocking diagnosis methods to general circulation models. Part I: a novel detection scheme. *Clim Dyn* 35:1373–1391. doi:10.1007/s00382-010-0767-5
- Barriopedro D, Fischer EM, Luterbacher J, Trigo RM, García-Herrera R (2011) The Hot Summer of 2010: Redrawing the Temperature Record Map of Europe. *Science* 332:220. doi:10.1126/science.1201224
- Bastos A, Gouveia CM, Trigo RM, Running SW (2014) Analysing the spatio-temporal impacts of the 2003 and 2010 extreme heatwaves on plant productivity in Europe. *Biogeosciences* 11(13):3421–3435. doi:10.5194/bg-11-3421-2014
- Bieli M, Pfahl S, Wernli H (2015) A Lagrangian investigation of hot and cold temperature extremes in Europe. *QJR Meteorol Soc* 141: 98–108. doi:10.1002/qj.2339
- Brunner L, Hegerl GC, Steiner AK (2017) Connecting atmospheric blocking to European temperature extremes in spring. *J Climate* 30:585–593. doi:10.1175/JCLI-D-16-0518.1
- Buehler T, Raible CC, Stocker TF (2011) The relationship of winter season North Atlantic blocking frequencies to extreme cold or dry spells in the ERA-40. *Tellus Ser A* 63:212–222. doi:10.1111/j.1600-0870.2010.00492.x
- Cattiaux J, Vautard R, Cassou C, Yiou P, Masson-Delmotte V, Codron F (2010) Winter 2010 in Europe: a cold extreme in a warming climate. *Geophys Res Lett* 37:L20704. doi:10.1029/2010GL044613
- Cattiaux J, Quesada B, Arakélian A, Codron F, Vautard R, Yiou P (2012) North-Atlantic dynamics and European temperature extremes in the IPSL model: sensitivity to atmospheric resolution. *Climate Dynamics* 40(9–10):2293–2310. doi:10.1007/s00382-012-1529-3
- Chan SC, Nigam S (2009) Residual diagnosis of diabatic heating from ERA-40 and NCEP reanalyses: intercomparisons with TRMM. *J Climate* 22(2):414–428. doi:10.1175/2008JCLI2417.1
- Christensen JH, Krishna Kumar K, Aldrian E, An S-I, I.F.A. Cavalcanti, de Castro M, Dong W, Goswami P, Hall A, Kanyanga JK, Kitoh A, Kossin J, Lau N-C, Renwick J, Stephenson DB, Xie S-P, Zhou T (2013) Climate phenomena and their relevance for future regional climate change. In: Stocker TF, Qin D, Plattner G-K, Tignor M, Allen SK, Boschung J, Nauels A, Xia Y, Bex V, Midgley PM (eds) *Climate change 2013: the physical science basis. Contribution of Working Group I to the Fifth assessment report of the intergovernmental panel on climate change*. Cambridge University Press, Cambridge
- Cohen J, Jones J (2011) A new index for more accurate winter predictions. *Geophys Res Lett* 38:L21701. doi:10.1029/2011GL049626
- Croci-Maspoli M, Schwierz C, Davies HC (2007) Atmospheric blocking: space-time links to the NAO and PNA. *Clim Dyn* 29:713–725. doi:10.1007/s00382-007-0259-4
- Davini P, Cagnazzo C, Neale R, Tribbia J (2012) Coupling between Greenland blocking and the North Atlantic Oscillation pattern. *Geophys Res Lett* 39(14):L14701. doi:10.1029/2012GL052315
- de Vries H, Haarsma RJ, Hazeleger W (2012) Western European cold spells in current and future climate. *Geophys Res Lett* 39:L04706. doi:10.1029/2011GL050665
- Deser C, Phillips AS (2009) Atmospheric circulation trends, 1950–2000: The relative roles of sea surface temperature forcing and direct atmospheric radiative forcing. *J Climate* 22(2):396–413. doi:10.1175/2008JCLI2453.1
- Fischer EM, Knutti R (2015) Anthropogenic contribution to global occurrence of heavy-precipitation and high-temperature extremes. *Nature. Climate Change* 5(6):560–564. doi:10.1038/nclimate2617
- García-Herrera R, Barriopedro D (2006) Northern Hemisphere snow cover and atmospheric blocking variability. *J Geophys Res Atm* 111(D21):D21104. doi:10.1029/2005JD006975
- García-Herrera R, Díaz J, Trigo RM, Hernández E (2005) Extreme summer temperatures in Iberia: health impacts and associated synoptic conditions. *Ann Geophys* 23:239–251
- García-Herrera R, Dias J, Trigo RM, Luterbacher J, Fischer EM (2010) A Review of the European summer heat wave of 2003. *Crit Rev Environ Sci Technology* 40(4):267–306. doi:10.1080/10643380802238137
- Gouveia CM, Bistinas I, Liberato MLR, Bastos A, Koutsias N, Trigo RM (2016) The outstanding synergy between drought, heatwaves and fuel on the 2007 Southern Greece exceptional fire season. *Agric For Meteorol* 218–219:135–145. doi:10.1016/j.agrformet.2015.11.023
- Green HK, Andrews N, Armstrong B, Bickler G, Pebody R (2016) Mortality during the 2013 heatwave in England—how did it compare to previous heatwaves? A retrospective observational study. *Environ Res* 147:343–349. doi:10.1016/j.envres.2016.02.028

- Haylock MR, Hofstra N, Klein Tank AMJ, Klok EJ, Jones PD, New M (2008) A European daily high-resolution gridded dataset of surface temperature and precipitation. *J Geophys Res* 113:D20119. doi:[10.1029/2008JD10201](https://doi.org/10.1029/2008JD10201)
- Hofstra N, Haylock M, New M, Jones PD (2009) Testing E-OBS European high-resolution gridded data set of daily precipitation and surface temperature. *J Geophys Res* 114:D21101. doi:[10.1029/2009JD011799](https://doi.org/10.1029/2009JD011799)
- Horton DE, Johnson NC, Singh D, Swain DL, Rajaratnam B, Diffenbaugh NS (2015) Contribution of changes in atmospheric circulation patterns to extreme temperature trends. *Nature* 522(7557):465–469. doi:[10.1038/nature14550](https://doi.org/10.1038/nature14550)
- Kalnay E, Kanamitsu M, Kistler R, Collins W, Deaven D, Gandin L, Iredell M, Saha S, White G, Woollen J, Zhu Y, Chelliah M, Ebisuzaki W, Higgins W, Janowiak J, Mo KC, Ropelewski C, Wang J, Leetmaa A, Reynolds R, Jenne R, Joseph D (1996) The NCEP/NCAR 40-year reanalysis project. *Bull Am Meteorol Soc* 77(3):437–471. doi:[10.1175/1520-0477\(1996\)077<0437:TNYP>2.0.CO;2](https://doi.org/10.1175/1520-0477(1996)077<0437:TNYP>2.0.CO;2)
- Kysely J, Plavcová E (2010) A critical remark on the applicability of E-OBS European gridded temperature dataset for validating control climate simulations. *J Geophys Res* 115:D23118. doi:[10.1029/2010JD014123](https://doi.org/10.1029/2010JD014123)
- Li J, Sun C, Jin F (2013) NAO implicated as a predictor of Northern Hemisphere mean temperature multidecadal variability. *Geophys Res Lett* 40(20):5497–5502. doi:[10.1002/2013GL057877](https://doi.org/10.1002/2013GL057877)
- Liu C, Tian B, Li K, Manney GL, Livesey NJ, Yung YL, Waliser DE (2014) Northern Hemisphere mid-winter vortex-displacement and vortex-split stratospheric sudden warmings: Influence of the Madden-Julian Oscillation and Quasi-Biennial Oscillation. *J Geophys Res Atmos* 119(12):12599–12620. doi:[10.1002/2014JD021876](https://doi.org/10.1002/2014JD021876)
- Lowe R, Ballester J, Creswick J, Robine JM, Herrmann FR, Rodo X (2015) Evaluating the performance of a climate-driven mortality model during heat waves and cold spells in Europe. *Int J Environ Res Public Health* 12(2):1279–1294. doi:[10.3390/ijerph120201279](https://doi.org/10.3390/ijerph120201279)
- Marcos R, Turco M, Bedia J, Llasat MC, Provenzale A (2015) Seasonal predictability of summer fires in a Mediterranean environment. *International Journal of Wildland Fire* 24(8):1076–1084. doi:[10.1071/WF15079](https://doi.org/10.1071/WF15079)
- Masato G, Hoskins BJ, Woollings TJ (2011) Wave-breaking characteristics of mid-latitude blocking. *Q J R Meteorol Soc* 138:1285–1296. doi:[10.1002/qj.990](https://doi.org/10.1002/qj.990)
- Monteiro A, Carvalho V, Gois J, Sousa C (2013) Use of “Cold Spell” indices to quantify excess chronic obstructive pulmonary disease (COPD) morbidity during winter (November to March 2000–2007): case study in Porto. *Int J Biometeorol* 57(6):857–870. doi:[10.1007/s00484-012-0613-z](https://doi.org/10.1007/s00484-012-0613-z)
- Muthers S, Matzarakis A, Koch E (2010) Summer climate and mortality in Vienna: a human-biometeorological approach of heat-related mortality during the heat waves in 2003. *Wien Klin Wochenschr* 122(17–18):525–531
- Pereira MG, Trigo RM, DaCamara CC, Pereira JMC, Solange ML (2005) Synoptic patterns associated with large summer forest fires in Portugal. *Agric For Meteorol* 129:11–25. doi:[10.1016/j.agrformet.2004.12.007](https://doi.org/10.1016/j.agrformet.2004.12.007)
- Pfahl S (2014) Characterising the relationship between weather extremes in Europe and synoptic circulation features. *Nat. Hazards Earth Syst. Sci.* 14: 1461–1475. doi:[10.5194/nhess-14-1461-2014](https://doi.org/10.5194/nhess-14-1461-2014)
- Pfahl S, Schwierz C, Croci-Maspoli M, Grams CM, Wernli H (2015) Importance of latent heat release in ascending air streams for atmospheric blocking. *Nature Geoscience* 8: 610–614. doi:[10.1038/ngeo2487](https://doi.org/10.1038/ngeo2487)
- Rex DF (1950a) Blocking action in the middle troposphere and its effect upon regional climate. Part I: an aerological study of blocking action. *Tellus* 2:196–211
- Rex DF (1950b) Blocking action in the middle troposphere and its effect upon regional climate. Part II: the climatology of blocking action. *Tellus* 2:275–301
- Ruti PM, Dell’Aquila A, Giorgi F (2014) Understanding and attributing the Euro-Russian summer blocking signatures. *Atmos. Sci. Lett.* 15(3): 204–210. doi:[10.1002/asl2.490](https://doi.org/10.1002/asl2.490)
- Santos JA, Corte-Real J (2006) Temperature Extremes in Europe and Large-Scale Circulation: HadCM3 future scenarios. *Climate Research* 31: 3–18. doi:[10.3354/cr031003](https://doi.org/10.3354/cr031003)
- Santos JA, Pinto JG, Ulbrich U (2009) On the development of strong ridge episodes over the eastern North Atlantic. *Geophys Res Lett* 36:L17804. doi:[10.1029/2009GL039086](https://doi.org/10.1029/2009GL039086)
- Santos JA, Wiillings T, Pinto JG (2013) Are the Winters 2010 and 2012 Archetypes Exhibiting Extreme Opposite Behavior of the North Atlantic Jet Stream? *Mon Weather Rev* 141(19):3626–3640. doi:[10.1175/MWR-D-13-00024.1](https://doi.org/10.1175/MWR-D-13-00024.1)
- Santos JA, Pfahl S, Pinto JG, Wernli H (2015) Mechanisms underlying temperature extremes in Iberia: a Lagrangian perspective. *Tellus Series A-Dynamic Meteorology Oceanography* 67:26032. doi:[10.3402/tellusa.v67.26032](https://doi.org/10.3402/tellusa.v67.26032)
- Seneviratne SI, Donat MG, Mueller B, Alexander LV (2014) No pause in the increase of hot temperature extremes. *Nature. Climate Change* 4(5):161–163. doi:[10.1038/nclimate2145](https://doi.org/10.1038/nclimate2145)
- Seo K, Lee H, Frierson DMW (2016) Unraveling the Teleconnection Mechanisms that Induce Wintertime Temperature Anomalies over the Northern Hemisphere Continents in Response to the MJO. *J Atmos Sci* 73(9):3557–3571. doi:[10.1175/JAS-D-16-0036.1](https://doi.org/10.1175/JAS-D-16-0036.1)
- Sillmann J, Croci-Maspoli M, Kallache M, Katz RW (2011) Extreme cold winter temperatures in Europe under the influence of north atlantic atmospheric blocking. *J Clim* 24(22):5899–5913. doi:[10.1175/2011JCLI4075.1](https://doi.org/10.1175/2011JCLI4075.1)
- Simolo C, Brunetti M, Maugeri M, Nanni T (2012) Extreme summer temperatures in Western Europe. *Adv Sci Res* 8:5–9. doi:[10.5194/asr-8-5-2012](https://doi.org/10.5194/asr-8-5-2012)
- Sousa PM, Trigo RM, Pereira MG, Bedia J, Gutiérrez JM (2015) Different approaches to model future burnt area in the Iberian Peninsula. *Agric For Meteorol* 202:11–25. doi:[10.1016/j.agrformet.2014.11.018](https://doi.org/10.1016/j.agrformet.2014.11.018)
- Sousa PM, Trigo RM, Barriopedro D, Soares PMM, Ramos AM, Liberato MLR (2016) Responses of European precipitation distributions and regimes to different blocking locations. *Clim Dyn.* doi:[10.1007/s00382-016-3132-5](https://doi.org/10.1007/s00382-016-3132-5)
- Treidl RA, Birch EC, Sajecki P (1981) Blocking action in the northern hemisphere: a climatological study. *Atmos Ocean* 19:1–23. doi:[10.1080/07055900.1981.9649096](https://doi.org/10.1080/07055900.1981.9649096)
- Trigo RM, Trigo IF, DaCamara CC, Osborn TJ (2004) Winter blocking episodes in the European-Atlantic sector: climate impacts and associated physical mechanisms in the reanalysis. *Clim Dyn.* 23:17–28. doi:[10.1007/s00382-004-0410-4](https://doi.org/10.1007/s00382-004-0410-4)
- Trigo RM, García-Herrera R, Díaz J, Trigo IF, Valente MA (2005) How exceptional was the early August 2003 heatwave in France? *Geophys Res Lett* 32:L10701. doi:[10.1029/2005GL022410](https://doi.org/10.1029/2005GL022410)
- Trigo RM, Ramos AM, Nogueira P, Santos FD, García-Herrera R, Gouveia C, Santo FE (2009) Evaluating the impact of extreme temperature based indices in the 2003 heatwave excessive mortality in Portugal. *Environ Sci Policy* 12:844–854. doi:[10.1016/j.envsci.2009.07.007](https://doi.org/10.1016/j.envsci.2009.07.007)
- van der Schrier G, van der Besselaar EJM, Klein Tank AMG, Verver G (2013) Monitoring European averaged temperature based on the E-OBS gridded dataset. *J Geophys Res Atmos* 118(11):5120–5135

- Woollings T, Pinto JG, Santos JA (2011) Dynamical evolution of north atlantic ridges and poleward jet stream displacements. *J Atmos Sci* 68(5):954–963. doi:[10.1175/2011JAS3661.1](https://doi.org/10.1175/2011JAS3661.1)
- Wright JS, Fueglistaler S (2013) Large differences in reanalyses of diabatic heating in the tropical upper troposphere and lower stratosphere. *Atmos. Chem Phys* 13:9565–9576. doi:[10.5194/acp-13-9565-2013](https://doi.org/10.5194/acp-13-9565-2013)
- WMO (2012) Cold spell in Europe and Asia in late winter 2011/2012. http://ane4bf-datap1.s3-eu-west-1.amazonaws.com/wmocms/s3fs-public/news/related_docs/dwd_2012_report.pdf